Blunt Trailing Edge Analysis of Supercritical Airfoils by a Navier-Stokes Code

Naoki HIROSE* and Nobuhiko KAMIYA**
NATIONAL AEROSPACE LABORATORY
Chofu, Tokyo, JAPAN

ABSTRACT

A preliminary analysis of flow about blunt trailing edge of NACA 0012 and supercritical airfoils in transonic speed was made utilizing a 2-D time-averaged Navier-Stokes code with turbulence model of Baldwin and Lomax. A very fine mesh distribution was focussed at the trailing edge region where conventional codes treat as sharp trailing edge with zero thickness. Computation was made for NACA 0012 airfoil with three kind of trailing edge thicknesses: cusp-type sharp, standard and 1% thickness and compared with the result of conventionally-treated trailing edge. 15% thickness supercritical airfoil with trailing edge thickness of 0.5% was also analyzed. It was found that a vortex shedding similar to the Karman vortices is formed and surface pressure near the trailing edge shows unsteady oscillation due the vortices. The magnitude and periodicity of the oscillation is governed by the bluntness. Also, it was shown that 'Kutta condition' is not necessarily satisfied for the blunt trailing edge.

1. Some Thoughts on Blunt Trailing Edge

It is well known that the trailing edge flow plays an important role on the lift and drag characteristics of an airfoil. A typical airfoil has sharp trailing edge. However, there are some well-known airfoils with a finite trailing edge thickness. Table 1 shows some of the examples. NACA 0012 has trailing edge thickness of 0.25%.

Most of the supercritical airfoils with rear loading pressure distribution will be included into this group. Whitcomb's airfoil[1] had very thin trailing edge when it was designed at first and then it was thickened later to alleviate structural problems without any penalty of subsonic drag level increase. GAW-2 [2] and LFC 73-06-135 [3] which are outgrowth of Whitcomb's airfoil have very thick trailing edge thickness of about one percent. More recently, Henne and Gregg [4] incorporated a positive utilization of thick trailing edge in their unconventional new airfoil concept of Divergent Trailing Edge airfoil. The last two airfoils: K 70-70-15 and K 800-441-13 in Table 1 are supercritical airfoils designed by Kamiya of NAL.[5]

Table 1. Examples of trailing edge thickness of typical airfoils

NACA 0012	0.002502
NACA 64A410	0.000420
RAE 2822	0.000090
G-K 75-06-12	0.0
Whitcomb	0.000500
GAW2	0.007090
LFC 73-06-135	0.001000
K 70-70-15	0.005220
K 800-441-13	0.005447

Blunt trailing edge is also used in turbine blade design. This, however, is due to thermal structural constraint and therefore the reasoning of utilizing the blunt trailing edge is different.

In the conventional theoretical analyses of airfoil, trailing edge thickness is regarded zero and sharp. Kutta condition is enforced for inviscid flow approximation. Even when an effective displacement thickness correction by boundary layer analysis is added, the circulation of external flow is computed with Kutta condition. The thickness of trailing edge and existence of non-zero width of wake are usually neglected. Recently Navier-Stokes (N-S) analysis is gaining popularity as the supercomputer became easy to access. Two-dimensional (2-D) N-S analysis can be made widthin a few minutes of computation. The viscous analysis by a 2-D N-S code alleviated the drawbacks of inviscid-boundary layer interaction approachs and it can handle the entire flowfield of the external flow, shock wave, boundary layer, separation and wake. The resolution in the direction normal to the airfoil surface is good in most cases of N-S analyses. However, mesh distribution along the surface is almost the same order as that used in potential and Euler analyses, i.e. the last mesh width at the trailing edge in the flow direction is about 0.5 to 1% of chord length. Therefore the actual blunt trailing edge is treated as a sharp trailing edge even in the N-S analysis. The sharp trailing edge treatment in the code enforces the flow dettach from trailing edge smoothly and 'Kutta condition' is automatically satisfied in the N-S analysis. This treatment does not give any particular inconveniences in the analysis and the aerodynamic characteristics data such as the global pressure distribution and lift and drag coefficients give Excellent comparison with the experimental data for practical purpose.[6,7]

A close examination of pressure distribution in the vicinity of the trailing edge in some airfoils indicates that 'Kutta condition' is not necessarily satisfied. Fig.1 shows a pressure distribution of K-70-70-15 Airfoil at the design point, M_∞= 0.70, α = 2.9° and C_L = 0.76. ○ is the experimental result at Re=20x10^6 obtained at NAL High Reynold Number 2-D Transonic Wind Tunnel.[8] Solid line is N-S analysis result computed at Re=1x10^6. The Reynolds number difference does not affect the pressure distribution significantly at the design point and the agreement between them is excellent except the level of supercritical region and shock wave location.

The Numerical result of the upper and lower surface pressure distributions crosses at the 95% chord station. The upper surface pressure monotonically recovers but the lower surface pressure expands due to the concave curvature behind 80% chord station until the trailing edge. The pressure recovers at the trailing edge because the flow meets with the upper surface flow there. There

* Branch Chief, Aircraft Aerodynamics Division
** Director, Advanced Aircraft Research Group

are numerical oscillations in the distribution because the mesh width along surface is large and about 2.5 % chord length and mesh inflexion is also large at the trailing edge. But this does not affect the result. The 'Kutta condition' is enforced at the first wake mesh next to the trailing edge mesh point where flow variables should have a unique physical set of values. The trailing edge point is doubly defined surface point where upper surface boundary condition is applied for the upperside flow and lower surface boundary condition for the lowerside flow. The 'computational trailing edge' is therefore located at one half mesh width further in the wake. Even if the trailing edge point is assumed to be a wake flow field point, the computational situation is almost same because these are out of the resolutionability scale of finite difference method.

The crossing of pressure curves and pressure behavier behind the crossing point is unusual. TSD and Euler analyses were also made(Fig.2 and 3). The crossing was not observed but it seems that Kutta condition enforces very strong pressure recovery very near the trailing edge. This will not be realized in the actual flow and flow separation may occur.

The experimental result only shows distributions until 95% chord station. Although they do not cross yet, they may cross at some station more closer to the trailing edge. The tendency of pressure distributions and their linear extrapolation support this conjection. Locating pressure taps very near to the trailing edge of the wind tunnel test model is very difficult. The trailind edge pressure measurement is therefore difficult also. If it can be made possible, the pressure value may be the avarage value of this region and the exact trailing edge pressure will not be obtained. Any further investigation was made to obtain the detailed pressure distribution near the trailing edge when this experiment was made many years ago.

K Airfoil was designed by an inverse potential design method developed by Ishiguro, et al.[9] The basic approach is based on Tranen's design method.[10] The examination of various airfoil design examples by Ishiguro's code shows that very sharp pressure recovery behind the 95% chord station is required to adjust to 'Kutta condition' in the design of rear loading type rear-cambered thick airfoil. The design(target) pressure distribution is realized in the most part of the airfoil but not near the trailing edge. When the boundary layer displacement correction is included in the design process, the boundary layer can not follow this strong adverse pressure recovery and flow separation occurs. Some measures to accomodate this separation in the design process such as the assumption of virtual linear pressure distribution are included in the analysis. Therefore the actual pressure distribution may be different from the one obtained from the design code.

Similar kind of pressure distribution was also found in designing a supercritical airfoil utilizing a design procedure[11] which iteratively uses a N-S solver and inverse design code of transonic integral equation of Takanashi.[12] In Case III design in Ref.11, the designed airfoil has a negative thickness in the region near the trailing edge although the geometry closes at the trailing edge. Therefore the thickness distribution is modified so as to thicken proportionally to $\delta_{TE}\sqrt{x}$. The modified airfoil has finite thickness distribution and the trailing edge thickness is $\delta_{TE}(=0.0025)$. The pressure distribution remains unchanged except in the trailing edge region where a small discrepancy appears due to the modification. The pressure curve crossing before the trailing edge appears. The modification does not affect the lift and drag coefficients significantly.

These examples suggest that the inviscid and N-S analyses give different pressure distributions in the trailing edge region. The flow measurement in the trailing edge region and wake in detail has been made by various investigators. Ref.13 summarizes some of typical airfoil experiments. Cook[14] gave a detailed measurement for RAE 2814 and 2822 airfoils. The measurement, however, does not include the details at the trailing edge. Cleary, et al.[15], Hurley, et al.[16] and Johnson, et al.[17] gave more detailed measurements on the trailing edge and near wake of supercritical airfoil. Ref.16 and 17 treat thick trailing edge flow of practical supercritical airfoils: DSMA 523 and 671. These airfoils are based on Whitcomb airfoil and have trailing edge thickness of about 1%. They show pressure distributions and velocity profiles near trailing edge. The pressure differs between the upper and lower

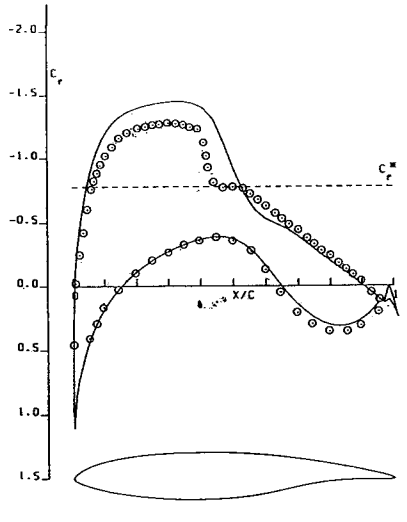

Fig.1 N-S Analysis of K-airfoil

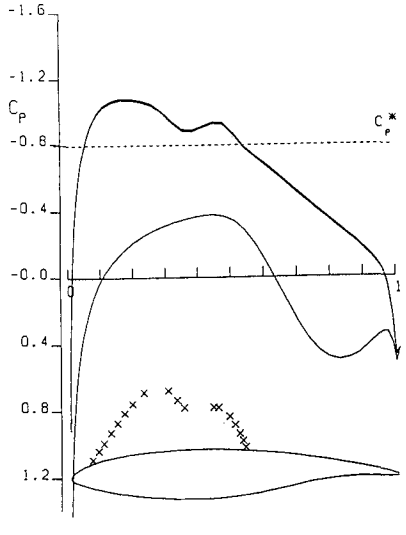

Fig.2 TSFOIL Analysis of K-airfoil

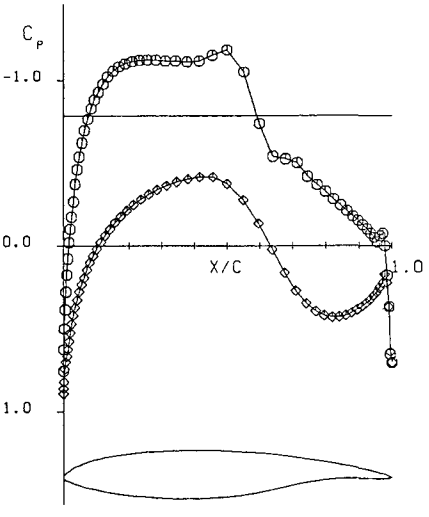

Fig.3 Euler Analysis of K-airfoil

sides of trailing edge. The direction and magnitude of velocity from upper side and lower side differs significantly at the trailing edge and even at the 105% chord station in the wake. These are time averaged profile measurement and unsteady quantities due to the bluntness and turbulence are not clarified yet. Although the present author has no experimental data on the detailed flow measurement in the trailing edge region in hand, these previous works suggest that it is not likely that the flows from both sides merge smoothly and satisfy 'Kutta condition'. A fundamental experimental research and implications for computational methods are also given by Thompson and Whitelaw[18].

2. Navier-Stokes Approach

The details of the trailing edge flow, however is not well clarified because the unsteady flow measurement of very small scale region of trailing edge area in wind tunnel experiment is very difficult to conduct. Instead, CFD tools may provide some clue to the understanding of the trailing edge flow, although turbulence model problem still remains.

As described in the previous section, conventional calculation by a N-S code does not provide any useful informations for trailing edge flow. The actual micro-scale flow in the trailing edge region of wing may be three-dimensional. Even a two-dimensional airfoil model flow may be in the same situation. However it will be justified that the flow is assumed as two-dimensional because span-wise vortex dominates the flow in the scale of trailing edge thickness. Also 2-D analysis is always the first step for understanding complicated flow phenomena. Therefore 2-D N-S approach is utilized in the present preliminary work.

The airfoil characteristics are dependent on thickness distribution, camber distribution and trailing edge angle as well as trailing edge thickness. The effects of these parameters are obtained even using inviscid code. The fundamental flow regime in micro-scale of trailing edge thickness is considered to be same. It is expected that a strong shear layer between the upper and lower surface boundary layer flows will be formed behind the trailing edge when a Navier-Stokes approach is applied. To capture this shear layer and its effect in micro-scale on the trailing edge flow, a very fine mesh distribution was focussed at the trailing edge region. A reasonable number of grid points was distributed along the airfoil surface to obtain the global pressure distribution rather than using a large number of grid points with very small mesh width same as used in the trailing edge region. A lot of computing time will be saved while obtaining the micro-scale flow motion.

Micro-scale trailing edge flow analysis by N-S code was also made by Schwamborn et al.[19] independently from present author. They adopted very fine mesh in the trailing edge region similar to the one in the present paper, however they pursued steady or time-averaged flow solution rather than time-dependent approach in the present work. Their interest rather lie on the evaluation of turbulence model. A brief description of the present work is already given at the same meeting[20]. The present paper gives the detail. Various ways of N-S approach is needed for understanding trailing edge flow.

3. Navier-Stokes Code

2-D N-S analysis code based on the implicit approximate factorization scheme for the time-averaged N-S equations was used[21]. Full viscous terms are included in the equations and in the numerical formulation rather than the thin-layer approximation because of the present aim of fine mesh analysis of trailing edge flow in detail. However, no comparison was made presently between the full and thin-layer N-S computations. Physical time step method was applied because the flow of concern will be unsteady type. The detail of the numerical method can be found in Ref.6.

4. Turbulence Model

The turbulence model used is the standard algebraic eddy viscosity model of Baldwin-Lomax's.[22] Fully turbulent computation was made assuming the flow is turbulent from the leading edge on both surfaces of airfoil. A relaxation model of eddy viscosity is also employed in the wake region. It is well known since the early days of N-S analysis that the effect of turbulence model is significant in transonic airfoil flow. Deiwert's pioneering work can be reffered.[23]

The length scale which appears in the formula of eddy viscosity coefficient is evaluated along η line normal to surface. The evaluation of coefficient has some ambiguity in definition. It is not rigorously defined and therefore is dependent on how the numerical description, programming and mesh distribution is used by individual investigators. Those code and mesh dependencies rather than the physical model differences has significant effects on the numerical result of the flowfield in the present state of art of the N-S analysis. These were not investigated this time although they should be clarified in the future work.

5. Airfoil Geometry

NACA 0012 airfoil is chosen as a typical conventional airfoil and K-70-70-15 airfoil is chosen as the supercritical airfoil example. Four types of trailing edge geometry are considered for NACA 0012 and two types for K-airfoil.

Table 2 lists the case names of the respective type geometry. Maximum thickness δ_{MAX} and trailing edge thickness δ_{TE} are shown. Geometry A11S is a standard NACA0012 with trailing edge thickness δ_{TE} of 0.00252. Here the chord length is taken as unity. A conventional mesh distribution in trailing edge region is made as shown later. The trailing edge point is treated as sharp corner point located at mean of upper and lower surface trailing edge ordinates. Mesh width is about 0.008 along surface and wake. Geometry A11R is same geometry as A11S except trailing edge shape. The trailing edge shape is modified to form a part of internally tangential circle. The trailing edge thickness is same and 0.00252. A11R is named 'Round Trailing Edge'. Geometry A12C has cusp-type sharp zero-thickness trailing edge. The thickness distribution along chord is modified from NACA 0012 by deducting

Table 2. Maximum and trailing edge thickness

Geometry	δ_{MAX}	δ_{TE}	Tail shape
A11S	0.120034	0.00252	Standard Open
A11R	0.120034	0.00252	Round T.E.
A12C	0.119280	0.0	Cusp T.E.
A14R	0.122270	0.01000	Round T.E.
K1S	0.15	0.00522	Standard Open
K1R	0.15	0.00522	Round T.E.

thickness proportionally to x. A12C is named 'Cusp Trailing Edge'. Geometry A14R has most thick trailing edge. Trailing edge thickness is 0.01 and it is rounded. Thickness distribution is given similar to A11R.

Geometry K1S is standard treatment of K-Airfoil. Maximum thickness is 0.15 and trailing edge thickness is 0.00522. Geometry K1R is same as K1S but trailing edge shape is rounded.

Among these geometries the trailing edge region behind 99.5% chord station is different shape of cylinder-type boat-tail or sharp edge in the modified geometries. Therefore, conventional treatment of N-S analysis only gives almost same result and will not provide any clue of significant effects of trailing edge thickness.

6. Grid Generation

A body-fitted automatic grid generation code AFMESH for airfoil analysis is used to construct the computing mesh for respective geometries. The method is based on the combination of poisson type ellyptic solver, geometric method and algebraic method. Clustering and adjustment are incorporated.

Table 3 shows the list of total mesh numbers, mesh number on airfoil(both surfaces) and on trailing edge, and size of computational region for respective geometries. The mesh number on airfoil other than trailing edge region is of the same order among geometries. Leading edge mesh width along surface, $\Delta\xi_{LE}$ is 0.0025. Minimum mesh width normal to surface, $\Delta\eta_{min}$ is 1×10^{-5}. In the trailing edge region, cusp and round trailing edge geometries has mesh width of $\Delta\xi_{TE}$ = 0.0004. Standard geometry has $\Delta\xi_{TE}$ =0.008. The computational region for NACA 0012 is limitted to 3 chord length in each direction to save computing time. Although small computational region gives significant far-field boundary condition effect on pressure distribution, it does not affect the flow behavier in trailing region because the region is same among geometries and global mesh distribution is similar to each other.

Computational meshes around airfoil are shown in Figure 4. Figure 4a is standard mesh for geometry A11S. Figure 4b is for round trailing edge geometry A11R. Very fine mesh is concentrated on the trailing edge region. Unfavorable skewed mesh is formed due to concentration. Figure 5a is standard mesh for K1S of K-Airfoil and 5b is mesh for K1R rounded trailing edge.

Table 3. Mesh numbers and computational region

Geometry	Mesh numbers (ξ x η)	Airfoil/T.E. meshes	Computational Region
A 1 1 S	125 x 45	93/ 0	X= -3 ～+4.2 Y= -3 ～+3
A 1 1 R	201 x 45	117/ 11	
A 1 2 C	201 x 45	117/ 0	
A 1 4 R	201 x 45	117/ 31	
K 1 S	125 x 51	93/ 0	X = -10 ～+10 Y = -10 ～+10
K 1 R	201 x 51	125/ 21	

$\Delta\xi_{LE}$ = 0.0025 , $\Delta\xi_{TE}$ = 0.0004 , $\Delta\eta_{min}$ = 0.00001

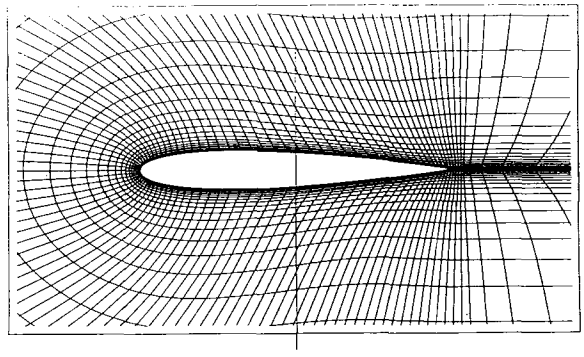

a. A11S geometry, 125× 45.

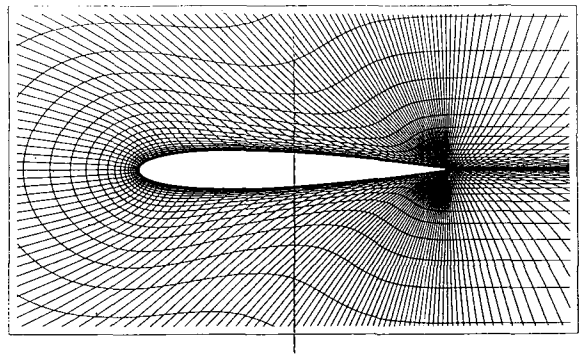

b. A11R geometry, 201× 45.

Fig.4 Computational mesh for NACA 0012.

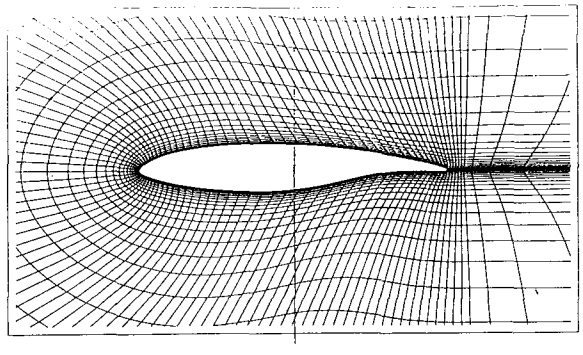

a. K1R geometry, 201× 51.

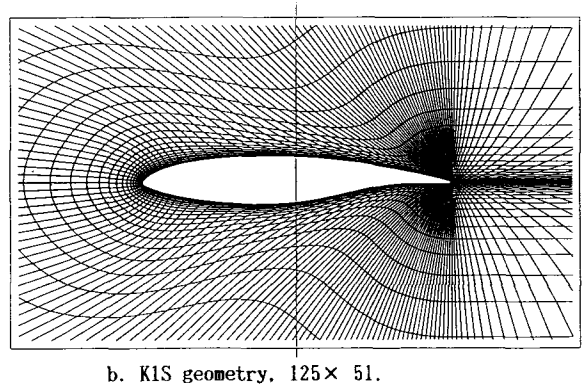

b. K1S geometry, 125× 51.

Fig.5 Computational mesh for K-Airfoil.

7. Results and Discussion

7.1. NACA 0012 Analysis

Computations at flow Mach number, $M_\infty=0.75$, angle of attack, $\alpha=0$ and Reynolds number $Re=1\times10^6$ are made for NACA 0012 airfoil on four types of computational mesh. Fully turbulent flow from leading edge is assumed. Flow with transition was also computed and similar trailing edge flow behavier was obtained. But turbulent boundary layer characteristics accompanying transition is strongly dependent on mesh arrangement and therefore only fully turbulent flow result is shown. All cases are computed using constant physical time step of $\Delta t=2^{-8}(=0.0039)$ until solution converges or stationary oscillative motion is reached. Normalized time elapsed is over 22 to 45.

Computed result are shown on Figures 6 to 11. Figure 6 shows pressure distribution curves: C_P vs. x and C_P vs. y for a. A11S standard mesh, b. A12C cusp trailing edge, c. A11R round trailing edge with standard thickness, and d. A14R with large trailing edge thickness. Pressure peak is supercritical in standard mesh computation but the rest of cases give subcritical pressure peak due to the mesh distortion. Except this, computation gives almost same results in global scale. Boundary layer displacement thickness at trailing edge is computed as about 0.01. The trailing edge thickness is about same order in geometry A14R and is smalier in other geometries.

Local pressure curve in trailing edge region, however, differs bewteen the standard and cusp or round cases. Standard case A11S converges to steady solution. Numerical oscillation at trailing edge is evident. It can be easily observed in C_P - y plot. Numerical oscillation causes flow separation at the last mesh point next to trailing edge located at 99.2% and at trailing edge point. The poor resolution of standard mesh hides actual physical flow behavier in trailing edge region.

Cusp trailing edge case A12C also converges to almost steady solution. The effective shape of trailing edge formed by mesh is similar to previous standard case but the mesh distribution is much denser than in the standard case. 17 mesh points are distributed along the last 1% of airfoil. The standard mesh only contains one point. Because of this local pressure curve in trailing edge region is monotonically increasing down to trailing edge. The trailing edge pressure is not fully recovered compared with standard case A11S. Figure 7 is enlarged plot of mesh from from 99% to 102% chord station and instantaneous velocity vector plot for respective geometries. Very small recirculating separated flow is found at trailing edge of cusp type A12C. Close check of boundary layer profiles reveals first separation occurs at x=0.978. The separation is unsteady and separated vortex moves down stream alternatively from both surfaces. The hight of separation is very thin order of at most 0.0003. Vortex shedding from trailing edge produce very small oscillation of pressure in trailing edge region which is not visible on Figure 6b and lift coefficient C_L is ±0.00008. Drag coefficient C_D

Table 4. Lift and drag coefficients (approximate value).

Geometry	C_L	C_D	C_{DP}	C_{DF}
A 1 1 S	0.00000	0.01574	0.006017	0.009725
A 1 2 C	±0.00008	0.02144	0.011985	0.009458
A 1 1 R	±0.0013	0.02152	0.011986	0.009535
A 1 4 R	±0.0025	0.02202	0.012284	0.009737

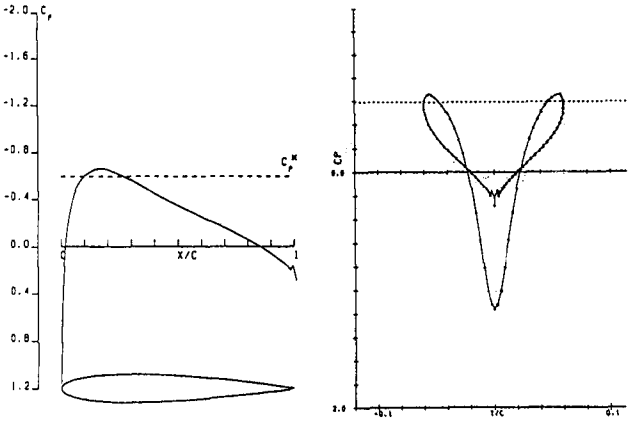

a. A11S, Standard mesh, $\delta_{TE}=0.00252$

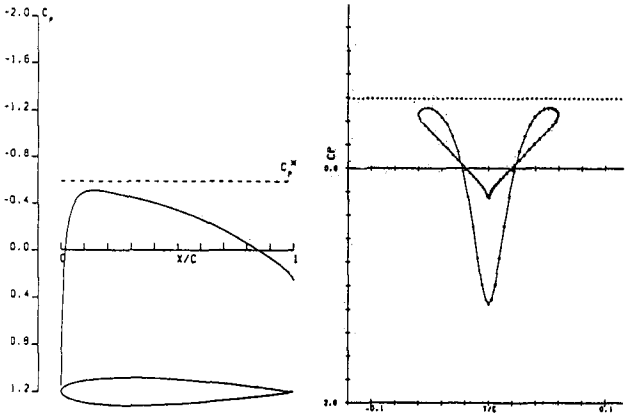

b. A12C, Cusp TE, $\delta_{TE}=0.0$

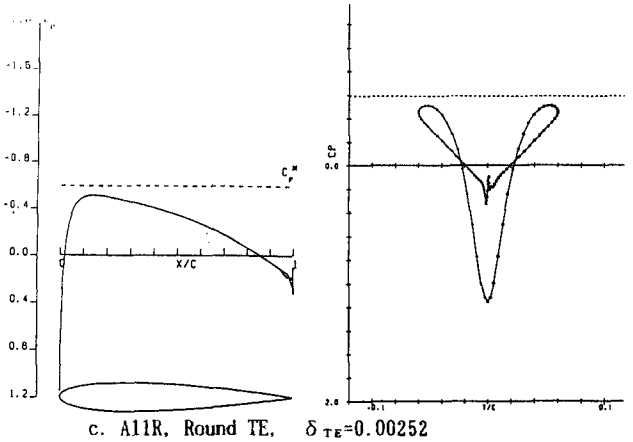

c. A11R, Round TE, $\delta_{TE}=0.00252$

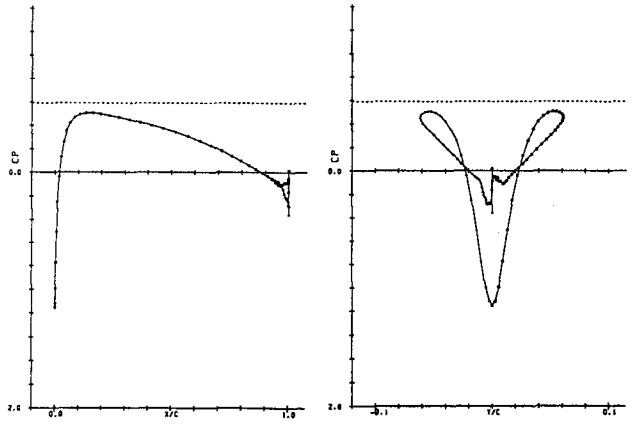

d. A14R, Round TE, $\delta_{TE}=0.01000$

Fig.6 Pressure distributions of NACA 0012 analysis.

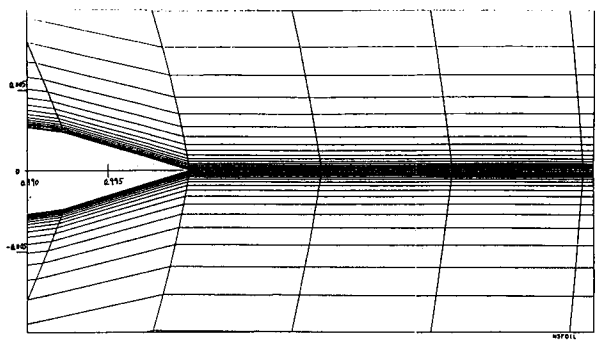

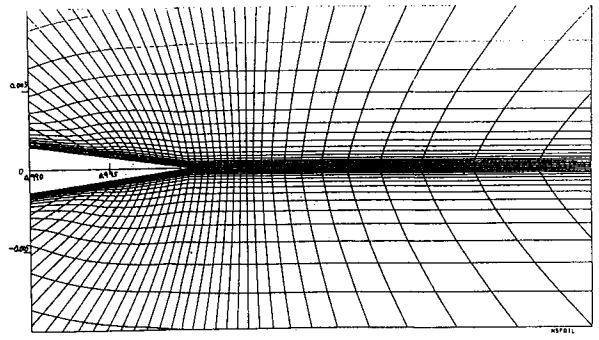

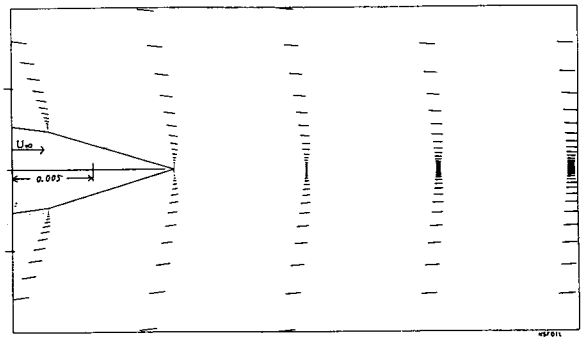

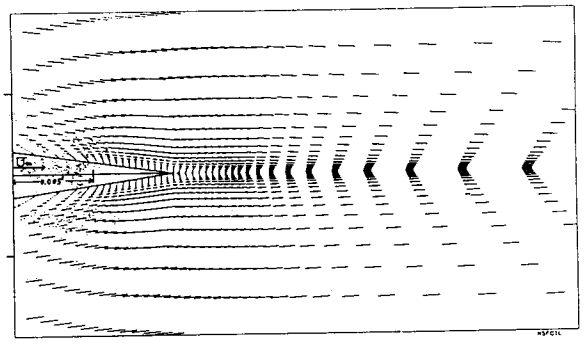

a. A11S, Standard mesh, δ_{TE}=0.00252

b. A12C, Cusp TE, δ_{TE}=0.0

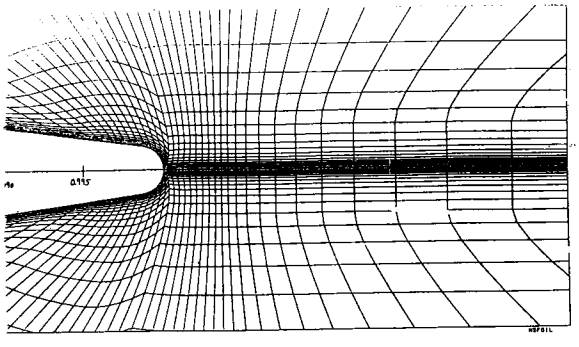

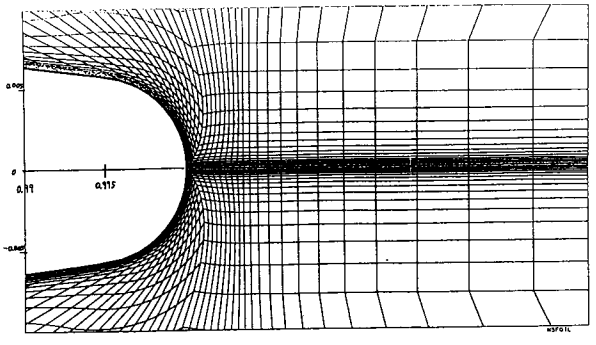

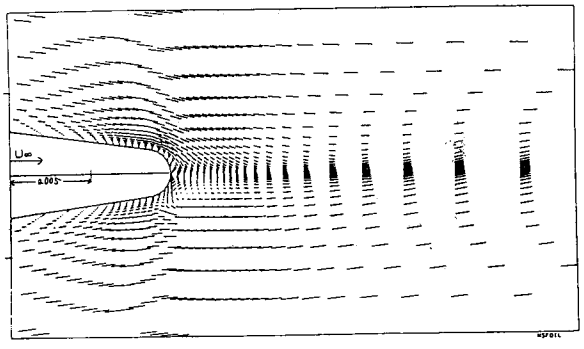

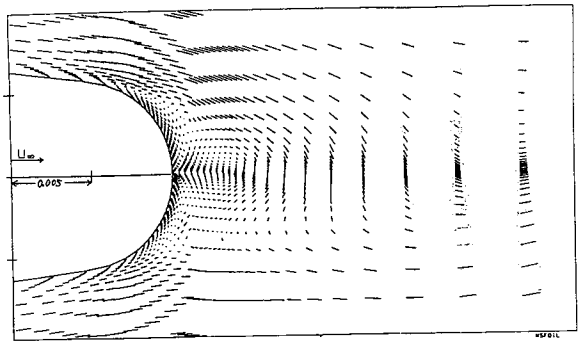

c. A11R, Round TE, δ_{TE}=0.00252

d. A14R, Round TE, δ_{TE}=0.01000

Fig.7 mesh and instantaneous velocity plot in trailing edge region of NACA 0012 analysis.

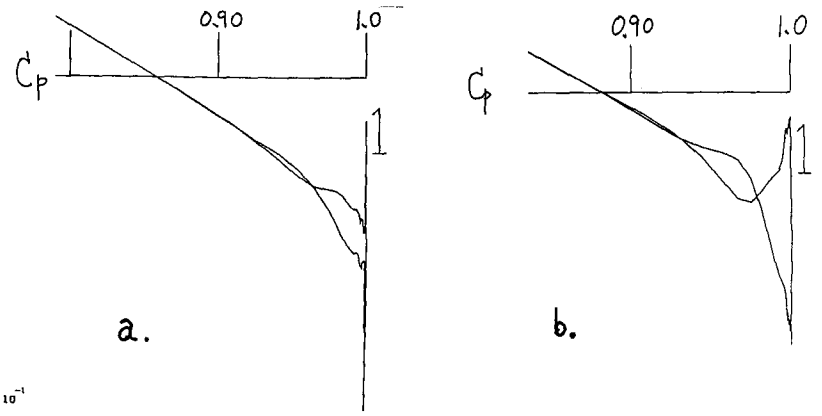

Fig.8 Instantaneous pressure distribution near trailing edge.

a. A11R, Round TE. δ_{TE}=0.00252 (left)
b. A14R, Round TE, δ_{TE}=0.01000 (right)

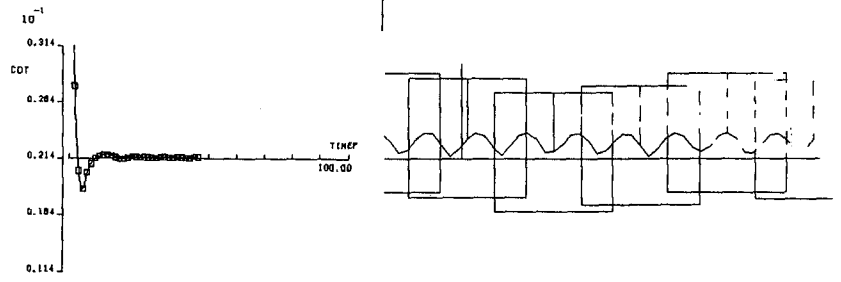

Fig.9 Drag coefficient vs. time.
A11R, Round TE, δ_{TE}=0.00252

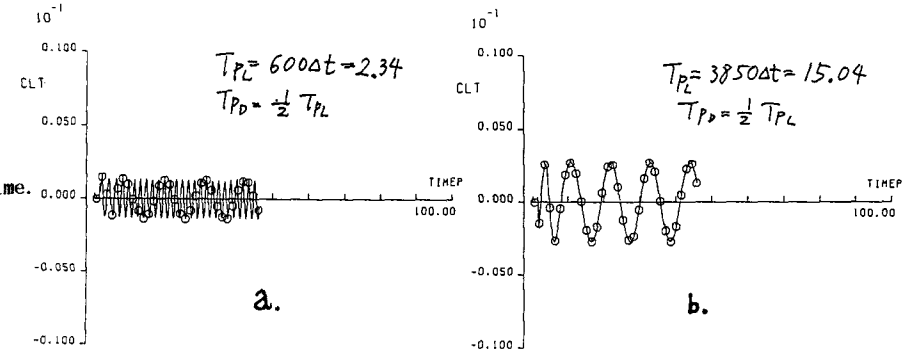

Fig.10 Lift coefficient vs. time.
a. A11R, Round TE.
δ_{TE}=0.00252 (left)
b. A14R, Round TE.
δ_{TE}=0.01000 (right)

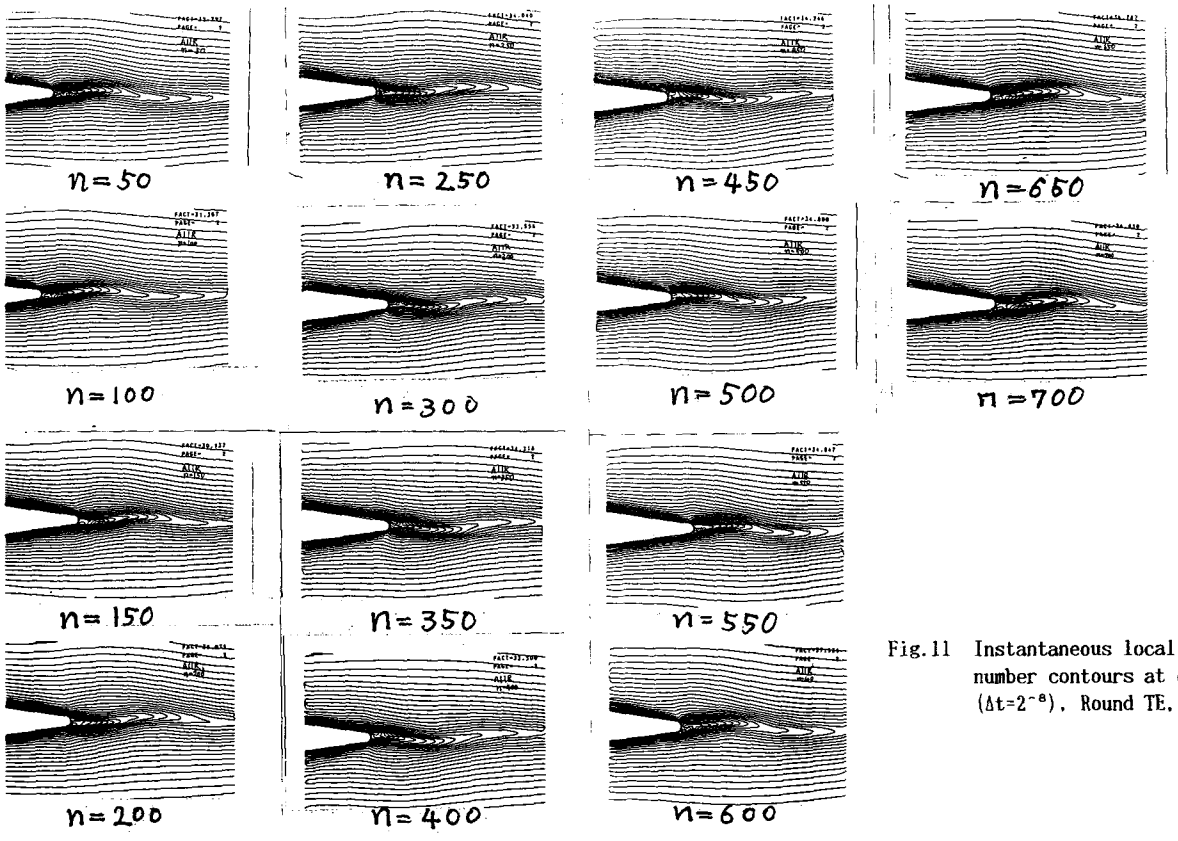

Fig.11 Instantaneous local Mach number contours at every 50 Δt ($\Delta t=2^{-8}$), Round TE, A11R.

is 0.02144 of which pressure drag C_{Dp} is 0.011985 and friction drag C_{DF} is 0.009458. Standard case A11S gives C_L is exactly 0.00000, C_D is 0.01574 (C_{Dp}=0.006017, C_{DF}= 0.009725). Table 4 shows results for four geometries. These numeric figures should not be considered as quantitatively reliable values because present computation is not well qualified due to various factors such as insufficient mesh numbers and numerical dissipations, etc. Only qualitative relative difference is meaningful. Difference of C_D comes mainly from C_{Dp}. Mesh skewness may be major factor. C_{DF} gives almost same value.

In case A11R, local pressure oscillation behind 95% station is significant as shown in Figure 6c. Case A14R shows oscillation is stronger than in A11R and the region extends further to upstream of about 90% station. Figure 8 shows enlarged pressure curves in trailing edge region of case A11R and A14R. C_p-y curve suggests non-negligible effect on drag characteristics. The velocity plots in Figures 7c and 7d show separation and vortices in wake. C_D vs. time for A11R is shown in Figure 9. The enlarged figure shows small stationary oscillation. C_L vs. time is in Figure 10 for A11R and A14R. The period of C_L oscillation, T_{PL} is 600Δt(=2.34) for A11R and 3850Δt(= 15.04) for A14R respectively. The period of C_D, T_{PD} is half of T_{PL}. Amplitude of C_L is $\pm$0.0013 for A11R and $\pm$ 0.0025 for A14R. The oscillation period T_{PD} is synchronized with each vortex shedding alternatively from blunt trailing edge. T_{PL} corresponds to one pair of vortices. The trailing edge region is entirely immersed in the boundary layer region. Reynolds number based on trailing edge thickness is 2.5 - 10 $\times 10^3$. The flow resembles Karman vortex shedding past a circular cylinder. Figure 11 shows instantaneous Mach number contours at every 50Δt for A11R. Vortex shedding is evidently observed. Similar result is also obtained in case A14R. Drag increase in order of cusp, standard round trailing edge and thick trailing edge. Both pressure and friction drags increase in this order. Present result gives qualitative behavier of unsteady blunt trailing edge flow, although significant effects of evaluating eddy viscosity remain.

7.2. Supercritical Airfoil Analysis

Computations at flow Mach number, M_∞=0.70, C_L=0.7 and Reynolds number Re=10x10^6 are made for K-Airfoil on standard and round trailing edge fine meshes. Fully turbulent flow is assumed. Time step and other parameters are same as in NACA 0012 analysis. Figure 12 shows pressure distributions. The skewed mesh gives too much smeared shock wave in round trailing edge analysis, K1R. Pressure profiles at several angles of attack are plotted in the figure. The rear load distribution is not affected at all by angle of attack. The pressure curve crossing always occurs in both cases. In K1R case, angle of attack is 1 degree to obtain C_L =0.7. These results is not satisfactory but will be useful to the present purpose of analysis. In standard case, numerical oscillation of pressure occurs at trailing edge and pressure is enforced to agree at trailing edge to satisfy Kutta condition. The solution is steady. In K1R case, pressure crossing also occurs but pressure fluctuates.

Figure 13 shows Machnumber contour for this angle of attack. Figure 14 is meshand velocity vector plot. The region is same as in the previous section. Figure 15 shows instantaneous pressure and Mach number contours. It is evident that vortex shedding is formed behind the round trailing edge. Small zig-zag of contour line is due to irregular mesh distribution. Pressure curve in trailing edge is shown in Figure 16. Time dependent lift coefficient and drag coefficient vs. time are shown in Figure 17. They fluctuate as a pair of vortices shed from trailing edge. The fluctuation has both of slow and high modes. The detail remains to be solved in future work.

8. Concluding Remarks

The present work only provides a preliminary analysis of blunt trailing edge flow using N-S code. Vortex shedding is found and surface pressure shows fluctuation due to vortices. The magnitude and periodicity is dependent on trailing edge thickness. It is likely Kutta condition is not necessarily satisfied in the micro-scale flow. Further detailed computation is needed for the understanding of trailing edge flow.

References

1. Whitcomb,R.T.,Review of NASA Supercritical Airfoils, ICAS Paper #74-10, (1974).
2. McGhee,R.J., Beasley,W.D. and Somers, D.M.,Low-Speed Aerodynamic Characteristics of a 13-percent-thick Airfoil Section Designed for General Aviation Applications,NASA TM X-72697, (1977).
3. Allison,D.O. and Dagenhart,J.R.,Design of a Laminar-Flow-Control Supercritical Airfoil for a Swept Wing, NASA CP-2036 Part I, pp.395-408, (1978).
4. Henne,P.A. and Gregg,R.D.,A New Airfoil Design Concept, AIAA Paper #89-2201-CP, (1989).
5. Kamiya, N., to appear on NAL Technical Report.
6. Kawai,N. and Hirose,N., Development of the Code NSFOIL for Analizing High Reynolds Number Transonic Flow around an Airfoil, NAL TR-816, (1984).
7. Hirose,N., Kawai,N. and Miyakawa,J.,Comparison of Transonic Airfoil Characteristics by Navier-Stokes Computation and by Wind Tunnel Test at High Reynolds Number, NAL TR-911T, (1986).
8. Takashima,K.,Experimental Works in the NAL High Reynolds Number Two-Dimensional Wind Tunnel on Advanced Technology and NACA Airfoil, ICAS Paper#82-5-4-4, (1982)
9. Ishiguro,T., Kamiya,N. and Kawai,N., Transonic Airfoil Design of Full Potential Flow, I.Numerical Procedure and Its Computational Examples, NAL TR-672, (1981).
10. Tranen,T.L.,A Rapid Computer Aided Transonic Airfoil Design Method, AIAA Paper #74-501, (1974).
11. Hirose,N.,Takanashi,S. and Kawai,N.,Transonic Airfoil Design Utilizing a Navier-Stokes Analysis Code, AIAA J. 25, No.3, pp.353-359, (1987).
12. Takanashi,S., Iterative Three-Dimensional Transonic Wing Design Using Integral Equations, J.Aircraft, 22, pp.655-660, (1985).
13. ---, Experimental Data Base for Computer Program Assessment, AGARD-AR-138, (1979).
14. Cook,T.A., Measurements of the Boundary Layer and Wake of Two Aerofoil Sections at High Reynolds Numbers and High-Subsonic Mach Numbers, ARC R&M No.3722, (1973).
15. Cleary,J.W., Viswanath,P.R.,Horstman,C.C. and Seegmiller,H.L., Asymmetric Trailing-Edge Flows at High Reynolds Number, AIAA Paper#80-1396, (1980).
16. Johnson,D.A.and Spaid,F.W.,Measurements of the Boundary Layer and Near Wake of a Supercritical Airfoil at Cruise Conditions, AIAA Paper #81-1242, (1982).
17. Hurley,F.X., Spaid,F.W., Roos,F.W.,Stivers,Jr.,L.S.

and Bandettini,A.,Detailed Transonic Flow Field Measurements about a Supercritical Airfoil Section, NASA TM X-3244, (1975).
18. Thompson,B.E. and Whitelaw,J.H., Trailing-Edge Region of Airfoils, J.Aircraft, 26, No3,pp.225-234,(1989).
19. Schwamborn,D.,Strykowski,P. and Oertel Jr.,H., Numerical Simulation and Physical Modelling of Transonic Trailing Edge Flow, Zierep,J.,Oertel,Jr.,H. (eds.),SYMPOSIUM TRANSSONICUM III, Springer Ver., pp. 121-130,(1988).
20. Hirose,N. and Takanashi,S., Computational Transonic Aerodynamics Research in Japan, Zierep,J.,Oertel,Jr.,H. (eds.),SYMPOSIUM TRANSSONICUMIII, Springer Ver., pp.33--47,(1988).
21. Steger,J.L., Implicit Finite-Difference Simulation of Flow about Arbitrary Two-Dimensional Geometries, AIAA J., 16, pp.679-686,(1978).
22. Baldwin,B. and Lomax,H., Thin-Layer Approximation and Algebraic Model for Separated Turbulent Flows, AIAA Paper #78-257,(1978).
23. Deiwert,G.S.,Computation of Separated Transonic Turbulent Flows, AIAA J., 14, pp.735-740,(1976).

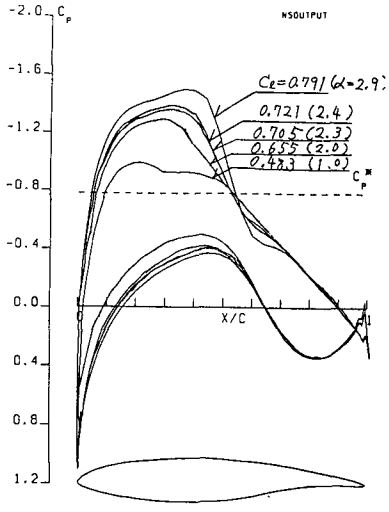

a. K1S, Standard mesh

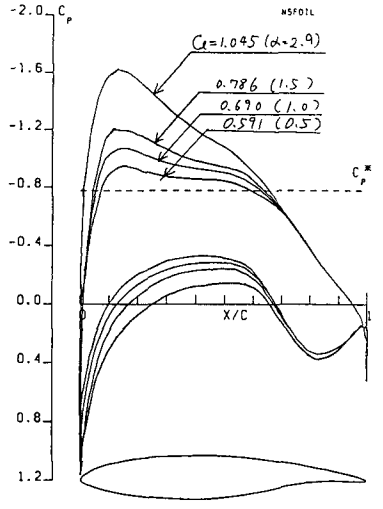

b. K1R, Round trailing edge

Fig.12 Pressure distribution of K-Airfoil

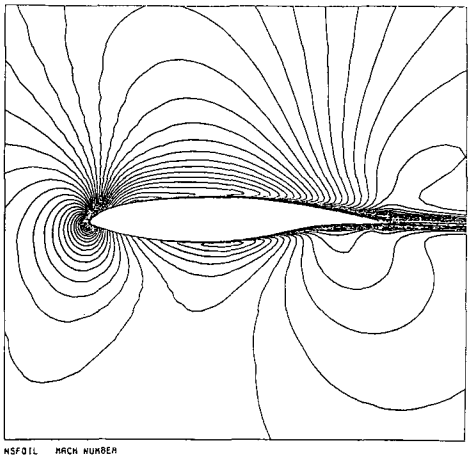

Fig.13 Mach number contour for K1R

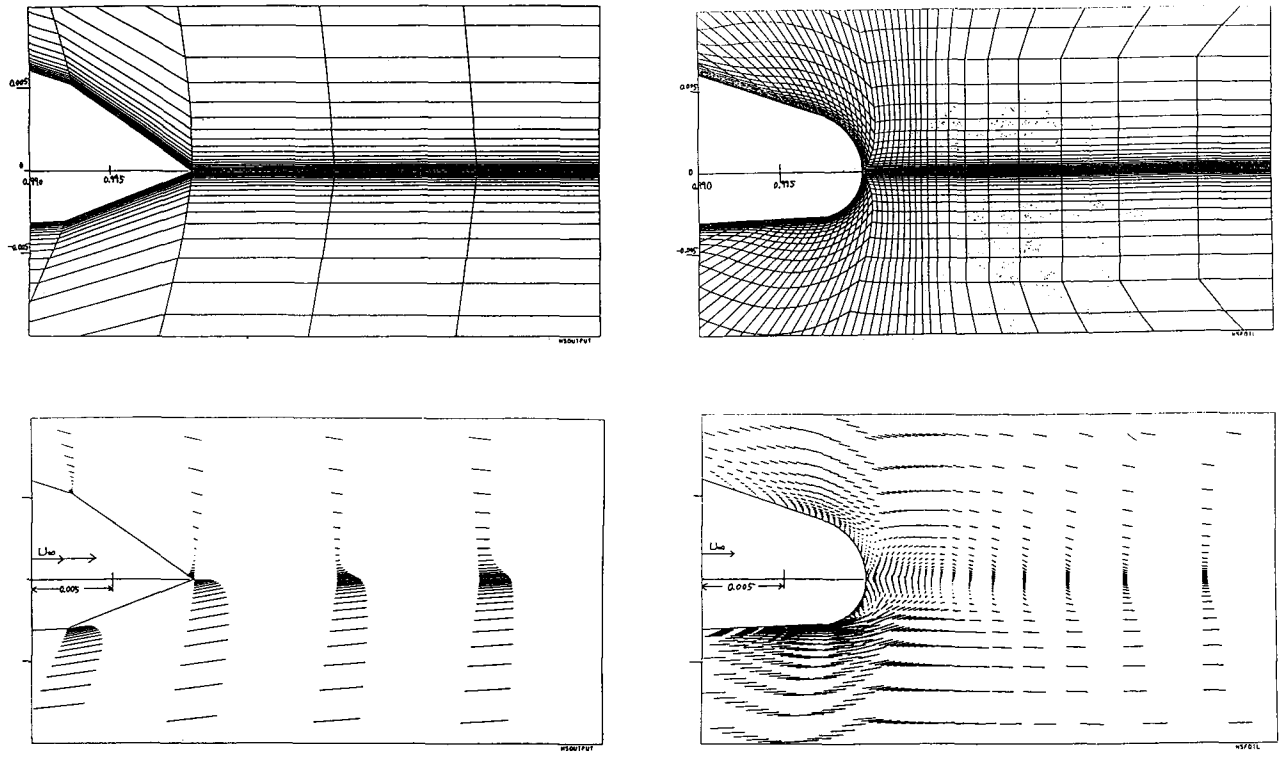

a. K1S Standard mesh b. K1R Round trailing edge

Fig.14 Mesh and instantaneous velocity plot in trailing edge region of K-Airfoil analysis.

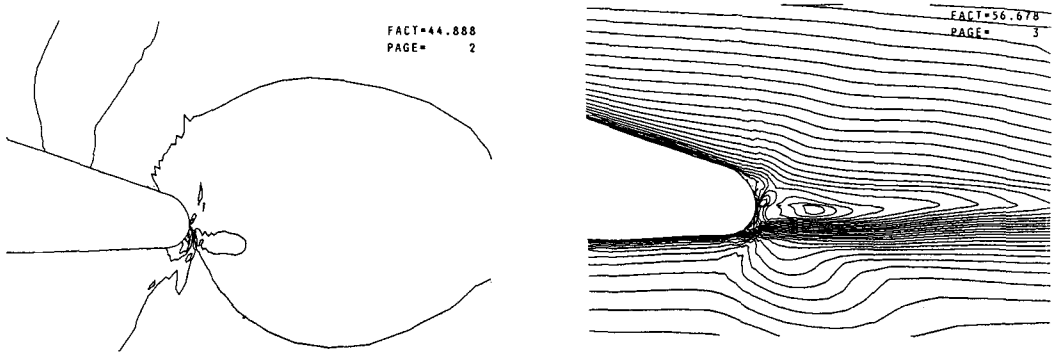

Fig.15 Instantaneous pressure contour (a) and Mach number contour (b).

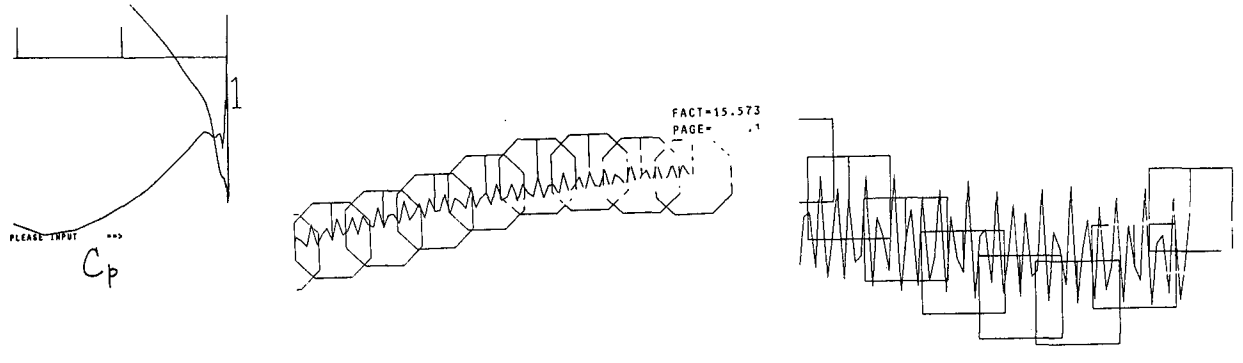

Fig.16 Instantaneous pressure near TE Fig.17 a. Lift Coefficient vs. time b. Drag Coefficient vs. time